

# TERRESTRIAL LASER SCANNER DATA DENOISING BY RANGE IMAGE PROCESSING FOR SMALL-SIZED OBJECTS

E. Smigiel\*, E. Alby, P. Grussenmeyer

Photogrammetry and Geomatics Group MAP-PAGE UMR 694, Graduate School of Science and Technology (INSA),  
24 Boulevard de la Victoire, 67084 STRASBOURG, France  
-(eddie.smigiel, emmanuel.alby, pierre.grussenmeyer)@insa-strasbourg.fr

**KEY WORDS:** Terrestrial Laser Scanning, Denoising, Modelling, Accuracy

## ABSTRACT:

The question of 3D data denoising has become a subject of intense research with the development of low cost acquisition systems. Recent works are based mainly on the adaptation of standard denoising methods historically developed in the context of image processing to a 3D point cloud or oftentimes on a 3D mesh. On one hand, methods which are independent from the acquisition stage are desirable since it allows to apply universal processes regardless from how the data were obtained. On the other hand, the noise which is to be removed or at least attenuated has specific origins; it also makes sense to get rid of it as close as possible to its physical origins, i.e. as early as possible in the global chain that goes from the acquisition to the final model. The paper addresses the question of Terrestrial Laser Scanner (TLS) data denoising. A method of denoising based on spatial filtering through wavelet decomposition is proposed. Its originality lies in the fact that it brings the problem back to the world of image processing. Each individual point cloud before registration is transformed into the corresponding range image which is the natural product of many TLS. Hence, TLS data denoising becomes a mere problem of image denoising. One can then envision to use the standardized image processing algorithms to process the point clouds before surface triangulation. In this paper, wavelet decomposition or more precisely speaking, subband coding is used to find out to what extent the important set of schemes deriving from the concept of subband coding is suited to the problem of TLS data denoising.

## 1. INTRODUCTION

Terrestrial Laser Scanners have been used for about ten years as a new tool in a wide variety of applications. Whatever the built-in technology (time of flight, phase shift, triangulation, etc.), the Signal to Noise Ratio (SNR) limits the accuracy of the point cloud and defines mainly the smallest object and the finest detail on the object which may be digitized adequately with a given instrument (Adami, 2007). Hence, the classical problem of data denoising remains relevant. For a given instrument which has been used at its best, i.e. its optimum resolution and accuracy conditions, what are the best post-processing methods which will allow one to obtain the maximum results? In other terms, what is the minimum size of the object and the minimum size of the detail on the object to be digitized provided one makes use of the extreme possibilities of the instrument combined with the most efficient post-processing methods?

This paper deals with this very general question through the example of a Terrestrial Laser Scanner based on the time of flight technology which is designed for architecture needs. Hence, the accuracy on the range is given by the constructor (as being equal to 7 mm in our case).

It will be shown that it is possible to denoise the point cloud by using the discrete 2D wavelet transform.

The paper is organized as follows: paragraph 2 gives a brief description of the standard industrial chain which goes from the acquisition of the point cloud to the final 3D model. Among others, the paper recalls some recent propositions of data denoising which is usually performed on the 3D registered

cloud or also on the 3D mesh. Paragraph 3 gives a very introductive description of data denoising by use of the so-called discrete wavelet transform starting with the 1D case and including some general ideas on 2D signals. In paragraph 4, it will be shown that the 3D data of TLS may be processed as images provided that one modifies slightly the standard chain. Then, experimental results are given. They show that the denoising scheme gives pretty good results by using standardized algorithms. Last, paragraph 5 suggests further developments since so far, the experimental results prove the interest of the principle of the method but have not allowed to establish the best parameters to choose.

## 2. THE STANDARD CHAIN: FROM ACQUISITION TO THE 3D MODEL

The standard chain from the acquisition of the data to the final 3D model consists in various stages whose order may often be changed as many variants exist. Besides, each stage may be realized by a wide variety of algorithms more or less automatically and is in itself a subject of research. The scope of this paragraph is to describe briefly the general idea of the standard industrial chain which has been implemented in most commercial softwares.

The acquisition provides the raw point clouds, i.e. sets of points given by at least their X, Y, Z coordinates and usually the intensity of the laser pulse and sometimes more information. Each point cloud corresponds to one position of the laser scanner, called a station, several stations being necessary to

---

\* Corresponding author.

obtain a satisfactory description of the object with a maximum amount of information.

Then, the different point clouds are registered and a unique point cloud is obtained for the whole object.

The next step consists in isolating the object of interest in the segmentation step.

Lastly, modeling or surface triangulation can be applied to obtain the mesh of the object. Further processing like texture mapping can still be applied depending on the final result one wants to obtain. This question of texture mapping is not central in this paper and will be neglected. Hence, the standard chain, illustrated on figure 1, will be defined until the mesh obtained by surface triangulation.

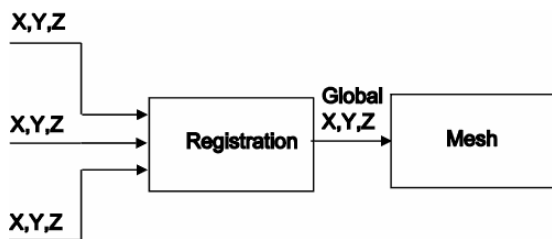


Figure 1. The standard chain from the individual point clouds to the final model

So far, the problem of denoising has been addressed through the processing of the 3D cloud or directly on the mesh. One can understand this approach which claims to be independent from the acquisition stage. Hence, the process becomes universal and one does not have to care for how the experimental data have been obtained. The first results which have been published were about the adaptation of standard isotropic methods well known in the image processing community to the 3D case of meshes. Historically, the classical Laplacian smoothing scheme has been developed (Gross, 2000; Ohtake, 2000). To overcome the oversmoothing problem due to lowpass filtering, Wiener filtering has also been adapted successfully to 3D meshes (Peng, 2001). A second group of methods, inspired by anisotropic diffusion has been developed (Taubin, 1995; Hildebrandt, 2004). Recently, Bilateral filtering has been introduced in the question of mesh denoising (Fleishman, 2003). Many variants and enhancements of these basic methods have been introduced. Theoretical works have shown some equivalences between these methods (Barash, 2002).

Though the care for acquisition independent methods is comprehensive, on the other hand, denoising as close as possible to the acquisition stage makes sense too for one can expect the noise to be more difficult to attenuate once cumulated in a complete 3D cloud obtained by merging of individual stations. Besides, adapting methods in the 3D case results in increased complexity, computation time and hardware resources.

The method we propose is based on 2D denoising based on wavelet decomposition or more precisely on subband coding.

### 3. WAVELET DENOISING

#### 3.1 Principle of wavelet denoising in the 1D case

Denoising by wavelet decomposition has been investigated for a long time, mainly since the works of Donoho *et al.* (Donoho, 1995). Though, it is far beyond the scope of this paper to describe the underlying theory, which may be considered as complicated for the non specialist, it may be interesting to give briefly the principal ideas which found the method and which may be understood quite easily provided that one has the basic knowledge in the mathematics of signal processing. However, the reader should not expect to have an exhaustive idea of the subtle questions which may arise and the many parameters and variants of the general method which exist and which are described in the adapted literature (Mallat, 1989; Vetterli, 1992).

The well-known results concerning the frequential representation of a signal which is related to the Fourier transform are used in the denoising task; indeed, the noise to be removed usually has some specific characteristics which may be expressed easily in the frequency domain. Frequential filtering consists in applying in the Fourier domain a low-pass filter which rejects the great majority of the white noise. This well-known technique has however some severe limitations. If the original signal contains some high frequencies, they will be filtered the same way as the white noise. This is referred as the smoothing effect of low-pass filtering.

To conclude with this very initial introduction, the classical scheme of denoising by low-pass filtering is not suited to signals which contain high-frequency components.

To overcome this difficulty, Donoho *et al.* have used the wavelet decomposition at the early 90s. Though, one speaks traditionally about wavelet denoising because of its parentry with wavelet theory, it would be much more accurate to talk about subband coding or multiresolution analysis of signals. Multiresolution analysis or subband coding consists in passing first the signal to be denoised in a pair of filters: a low-pass filter that results in the approximation part of the original signal and a high-pass filter that results in the detail part of the signal as represented on figure 2.

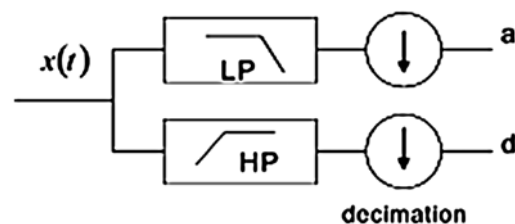


Figure 2. First level decomposition of signal

Theoretical arguments show that these two parts of the signal may be downsampled by a factor two or decimated without losing any information. Hence, the signal is represented by its two parts, the approximation and the detail by a total amount of samples that is exactly the original amount of points in the original signal. The samples of the approximation and the detail are called the coefficients of the decomposition. It is beyond the scope of this paper to show how this subband coding or multiresolution is connected to wavelet theory. The only intuitive result to be known is that subband coding represents a

discrete wavelet transform and that the wavelet family to be used (Haar, Coifmann, Daubechies for instance) is deeply connected to the transfer functions of the low and high pass filters that are used in the decomposition. The reconstruction task consists in passing the two parts (approximation and detail) through what is usually called quadrature mirror filters to obtain without any modification the original signal. The denoising task is going to be performed by the modification of one part of the decomposed signal (actually, the detail) before the reconstruction task. However, before getting to that point, let us describe the multi-level decomposition. The idea is to split the approximation part into two components according to the same scheme as before. A low-pass filter applied on the approximation allows to obtain the approximation of the approximation and a high-pass filter allows to obtain the detail part of the approximation. One can carry on the decomposition to further levels. Since each filter is followed by a downsampling stage (a factor 2), it is quite easy to understand that the representation consists in exactly the same amount of point as the original signal in the direct space. Hence subband coding consists in cutting the frequency domain into the so-called dyadic transform since each band is cut one step further into two bands so that each band is a  $\frac{1}{2^n}$  fraction of the frequency bandwidth,  $n$  being the level of decomposition. Figure 3 represents a level 3 decomposition of a signal.

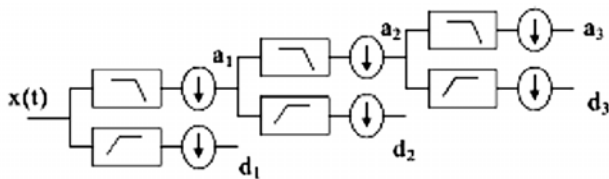


Figure 3. Level 3 decomposition of a signal

The denoising method is based on the modification of the detailed parts of the multiresolution analysis. To figure out how the method works, a good example is probably better than a long theoretical explanation. The original noisy signal shown on figure 4 is taken from one of the historical articles of Donoho *et al.* It consists in a NMR (Nuclear Magnetic Resonance) spectrum which exhibits sharp transitions, i. e. high-frequency components. If one uses the classical low-pass filtering to reduce noise, these high-frequency components are going to be modified too and the denoised signal will be smoothed too much.

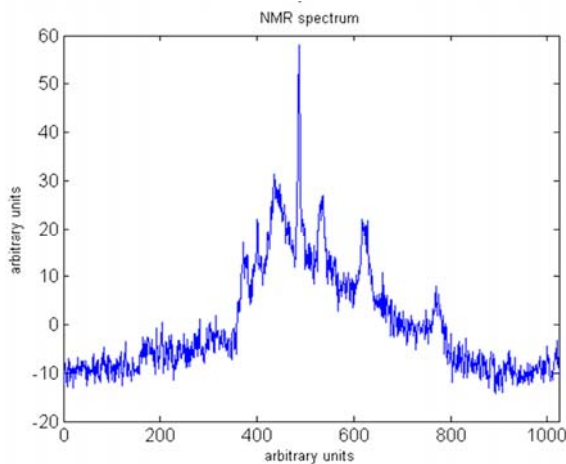


Figure 4. The noisy data (NMR spectrum) taken from Donoho *et al*

Figure 3 shows the decomposition at level three which leads to the signal being expressed by:

$$x(t) = a_3 + d_3 + d_2 + d_1$$

The denoising method acts on the detailed parts. The idea is to set up one threshold per detail and to retain only the coefficients which exceed these thresholds and to put the other ones to zero.

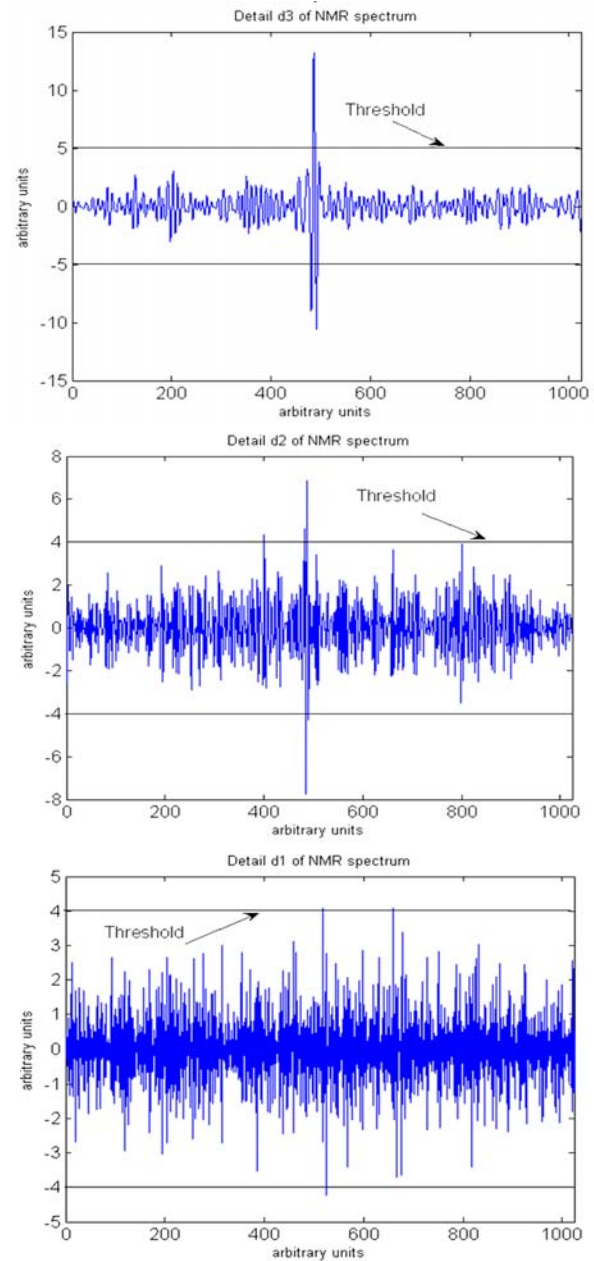


Figure 5. Details and corresponding thresholds of the noisy NMR

Indeed, the coefficients in between the symmetrical thresholds are likely to be part of the noise whereas the coefficients that are beyond these thresholds are likely to be part of the actual signal when this latter varies quickly. In other words, the decomposition allows to retain in the high frequencies the part

of the signal which varies on a great amplitude since these variations are likely to be part of the actual signal.

The adapted thresholds are shown on each detailed part of the decomposition shown on figure 5. Last, figure 6 shows the denoised signal obtained after reconstruction. The sharp peaks have been conserved but the noisy part of the signal has obviously been reduced.

Hence, the method may be seen as a fine analysis band by band to identify where the actual components of the signal are located compared to the noise which is supposed to be spread over the whole range of frequencies. These actual components are identified every time they have an amplitude great enough so that they may be conserved. It is obvious then that some actual components are removed along with the noise whenever their amplitudes can not be isolated from the surrounding noise. Thus, the threshold has to be adapted through a trade-off between loosing too much actual signal or keeping too much noise. The reader may investigate further important topics like for instance the different natures of thresholds (soft or hard), how they can be determined, or the optimum level of decomposition.

The ideas developed in the former paragraph can be generalized to 2D signals which are generally called, images. Indeed, an image, on a mathematical point of view is a function of two variables. Oftentimes, the physical nature of the function is the intensity as being function of the two space variables in the Cartesian frame. When it comes to digital images, one talks about the intensity of each pixel as function of the two coordinates which are sampled on a rectangular and regular grid. However, on a more general point of view, the physical natures of both the function and its two variables do not matter.

Denoising images by low-pass filtering leads to the same drawbacks as in the 1D case exposed above. The high-frequency part of the noised is removed or at least attenuated but so is the high-frequency part of the actual signal. It results in the well-known smoothing effect. If the actual image exhibits sharp transition of the intensity, i. e. contains high-frequency components, they are going to be smoothed and the filtered image damaged.

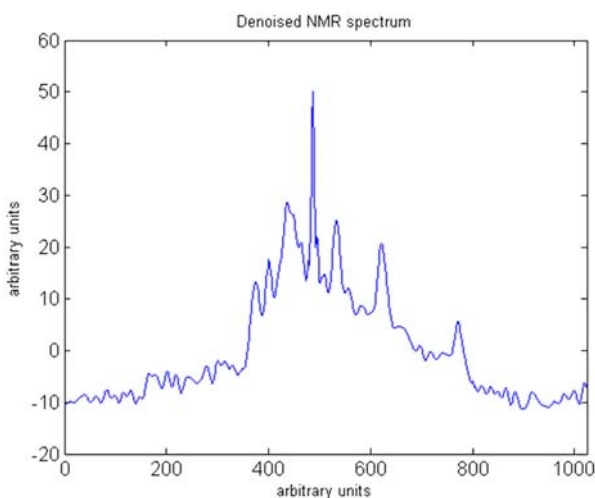


Figure 6. Denoised NMR spectrum

Denoising images by a 2D wavelet transform has been investigated a lot. The ideas exposed in the former paragraph, the multilevel decomposition through low-pass and high-pass filters leading to approximations and details of the image, the thresholding of the detailed parts and reconstruction to obtain finally the denoised image, generalize easily to the 2D case. The main difference compared to the 1D case is that the detail part of the decomposition at level  $n$  is composed of three sub-images, the horizontal detail, the vertical detail and the diagonal detail which are obtained by three high-pass convolution kernels that extract the high-frequency components of the image in these respective directions. Figure 7 shows the decomposition at level 2 of the well-known 'lena' image which has been used as a standard image to illustrate image processing but also to measure the performance in denoising and compression schemes within the image processing community.



Figure 7. Level 2 decomposition of the famous 'lena'

#### 4. RANGE IMAGE DENOISING BY WAVELET TRANSFORM

##### 4.1 The image approach

In the state-of-the-art methods briefly described above, the input data is either a global point cloud or a surface mesh. The methods developed, though successful, are not standardized yet and not easy to implement. The approach that has been developed for this paper which is based on a previous work (Smigiel, 2007) consists in coming back to the standard chain at the point where one does not have to deal with 3D data, i.e. on the very basic principle of laser scanning. The scanning consists in sweeping both the horizontal and vertical angle, respectively  $\theta$  and  $\varphi$ : for each position of the laser beam, the range,  $R$  is measured. Hence, the coordinates of the measured point are given in the spherical frame tied to the laser by the triplet  $(R, \theta, \varphi)$ . It may thus be considered that the data obtained by the laser for one station is a 2D function  $R(\theta, \varphi)$ . If the scanning is rectangular, then this 2D function is nothing else but an image in the very classical sense with the exception that the intensity information (being function of two space variables) is replaced

by range. Thus, spatial filtering of the point cloud may be processed as a mere image filtering with all the methods that have been developed within the image processing community. The standard chain exposed in figure 1 is then preceded by the one shown on figure 8.

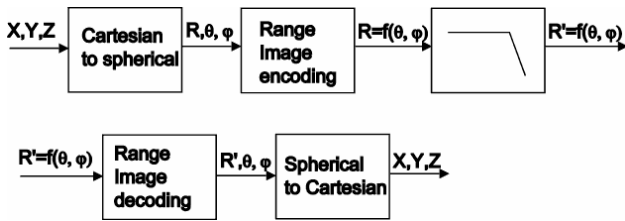


Figure 8. The filtering chain ahead of the standard chain of figure 1. The chain is applied for each station before registration.

The raw point cloud from one station given by the (X,Y,Z) coordinates is first transformed into the (R, θ, φ) triplet (the laser scanner measures directly these values but transforms them into their X,Y,Z equivalent and outputs them in the output file). Then the (R, θ, φ) set is transformed into an image with a rectangular grid by exploiting the Δθ and Δφ information of the scan. The filters are applied and the inverse transformations are applied to come back to the X,Y,Z space. Then, these modified (X,Y,Z) clouds may enter the standard chain described on figure 1; the individual clouds that have been the objects of the former filtering are registered, the registered cloud is segmented and finally enters the surface triangulation step. Hence, denoising the point cloud becomes merely a question of image denoising.

#### 4.2 Results

The general aim of this research being to find out to what extent architectural TLS may be used to scan small objects, the method has been applied on blocks of Corinthian capitals found in Mandeure, a gallo-roman city in the East of France. The volume of these capitals is a fraction of one cube meter which is quite small compared to the usual objects that are digitized with an architectural TLS. To quantify the noise reduction, different methods may be applied. As the final goal of 3D digitization, the visual quality of the final mesh is the central issue. However, for objects with complex geometry, it is not an easy task to control noise reduction on the final mesh on a quantitative basis. Thus, a first test consists in modelling simple geometrical objects (planes, spheres) before and after noise reduction and to compare the standard deviation of the point set.

The experimental data have been acquired with a Trimble GX TLS using time-of-flight technology with the following parameters:

The vertical resolution and the horizontal resolution have been set to 50mm at 100m for an average scan distance of about 8m. Each point has been acquired through 25 laser shots in order to increase the accuracy of the range measure.

The blackboard which has been put into the scanned scene has been modelled with the following results. Before wavelet denoising, the standard deviation around the mathematical plane is 1.7mm and after wavelet denoising, it has been decreased to 0.27 mm. The standard deviation ratio is thus close

to 6 which can be considered as a nice result. The “thickness” of the point cloud has been reduced by a factor 6. However, as a plane does not contain high frequencies, this result can not in itself justify the method.

That is why we have also modelled the 38.1 mm radius spheres which are used for cloud registration before and after denoising. The table below shows the three coordinates of the modelled sphere centre before and after denoising and in the last column the standard deviation of the points of the cloud which have been used for sphere modelling. One can see that the denoising scheme does not affect the sphere position which is an important result. Indeed, the spheres being used for registration of the individual point clouds, any displacement of a sphere centre would prevent the registration stage to be operated correctly. However, the result concerning the standard deviation is not clear. For one of the experimented spheres, the standard deviation decreases a little bit whereas for the two others, things are getting worse. Hence, the test with spheres is quite deceiving. This could be explained by a poor choice of the thresholds that have been used and that would not fit the spheres. The last test which may be done consists in modelling a real point cloud obtained by scanning a real object before and after denoising. The test has been applied on an archeological object consisting in a Corinthian capital block shown on figure 9 and 10. A simple mesh using the Delaunay triangulation on the complete set of points has been applied without any post-processing to evaluate to what extent our denoising scheme improves the final model.

Before denoising, the triangulation results in a disturbed surface whereas after denoising, the global surface appears smoother without having lost the sharp edges of the object. In particular, one may notice the almost square hole at the bottom of the object whose edges have not been affected by denoising.

Sphere #1	Center position X (mm)	Center position Y (mm)	Center position Z (mm)	Standard deviation (mm)
Before denoising	1208.70	-9248.79	287.13	1.54
After denoising	1209.07	-9249.21	287.28	0.95

Sphere #2	Center position X (mm)	Center position Y (mm)	Center position Z (mm)	Standard deviation (mm)
Before denoising	1215.59	-8741.91	-168.52	1.53
After denoising	1215.96	-8742.02	-168.61	1.83

Sphere #3	Center position X (mm)	Center position Y (mm)	Center position Z (mm)	Standard deviation (mm)
Before denoising	504.49	-8333.58	-744.85	1.40
After denoising	504.12	-8333.34	-744.65	2.35

#### 5. CONCLUSION AND FURTHER WORKS

In this paper, we have shown the feasibility of the method which consists in denoising the TLS data through the range image. The first advantage consists in the availability of many

image processing based denoising schemes, subband coding being just one of them. The second advantage lies in the fact that one can always expect interesting results when denoising as close as possible to the physical measurement. Hence, denoising the data before registration makes sense.

However, many further questions have to be answered. Firstly, concerning wavelet denoising, there exist many variants to the general concept: for instance, the question of the mother wavelet to use depending on the object to digitize is still open. Besides, the question of the values of the threshold to set is also to be solved. To conclude with the question of wavelet denoising, other extensions of the general method could also be studied like for instance wavelet packet decomposition which consists in decomposing the detailed part of the signal into its approximated part and detailed part which could help to identify better where the useful components of the signal are located to distinguish more efficiently between noise and signal.

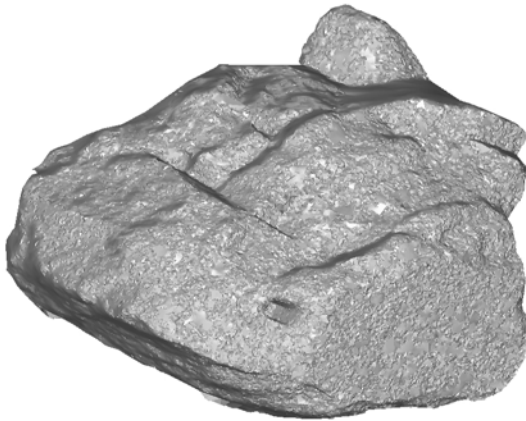


Figure 9. Mesh obtained by Delaunay triangulation on the raw point cloud

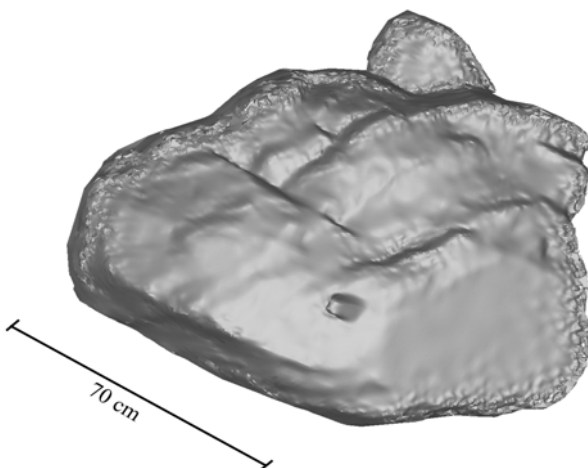


Figure 10. Mesh obtained by Delaunay triangulation on the denoised point cloud

Secondly, in the recent years, new image denoising methods have appeared like the so-called anisotropic diffusion methods or NL-means. It would be interesting to find out to what extent, they would be suited in the case of range image denoising.

Lastly, the authors are aware that so far, the work is quite prospective. In the near future, the processing of complete experimental sets from the initial point clouds up to the final model will be done on raw range images and the corresponding denoised images to compare the results on a quantitative basis.

## REFERENCES

### References from Journals:

Fleishman, S., Drori, I., Cohen-Or, D., 2003. Bilateral Mesh Denoising. *ACM Trans Graphics*, vol. 22, pp. 950-953.

Barash, D., 2002. A fundamental relationship between bilateral filtering, adaptive smoothing and the nonlinear diffusion equation. *IEEE Trans. Pattern Analysis and Machine Intelligence*, vol. 24, no. 6.

Donoho, D. L., 1995. Denoising by soft thresholding. *IEEE Trans. Inform. Theory*, vol. 41, pp. 613-627.

Mallat, S., 1989. A theory for multiresolution signal decomposition: the wavelet representation. *IEEE Trans. Patt. Recog. and Mach. Intell.*, vol. 11, pp. 674-693.

Vetterli, M., Herley, C., 1992. Wavelets and filter banks: Theory and design. *IEEE Trans. Signal Process.*, vol. 40, pp. 2207-2232.

### References from Other Literature:

Gross, M., Hubeli, A., 2000. Fairing of nonmanifolds for visualization. *Proceedings of IEEE Visualization*, 407-414.

Ohtake, Y., Belyaev, A. and Bogaeski, I., 2000. Polyhedral surface smoothing with simultaneous mesh regularization. *Proceedings of Geometric Modeling and Processing*, 229-237.

Peng, J., Strela, V., Zorin, D., 2001. A simple algorithm for surface denoising. *Proceedings of IEEE Visualization*, pp. 107-112.

Taubin, G., 1995. A Signal Processing Approach for Fair Surface Design. *SIGGRAPH '95 Conf. Proc.*, pp. 351-358.

Hildebrandt, K., Polthier, K., 2004. Anisotropic Filtering of Non-Linear Surface Features. *Eurographics '04*, vol. 23, no. 3.

Smigiel, E., Callegaro, C., Grussenmeyer, P., 2007. Digitization of the collection of moldings of the university Marc Bloch in Strasbourg: a study case. *XXI International CIPA Symposium*, 2007, pp. 674-679.

Adami, A., Guerra, F., Vernier, P., 2007. Laser scanner and architectural accuracy test. *XXI International CIPA Symposium*, 2007, pp. 7-11.